CORNER STRESS ANALYSIS OF JOINTED CONCRETE PAVEMENTS

Ying-Haur Lee, Assoc. Prof., Dept. of Civil Eng., Tamkang Univ., Taiwan, R.O.C.
Ying-Ming Lee, Research Assistant, Dept. of Civil Eng., Tamkang Univ., Taiwan, R.O.C.

ABSTRACT

Since corner breaks are one of the major structural distresses in jointed concrete pavements, the ILLI-SLAB finite element (F.E.) program was used to analyze the critical corner stresses of concrete pavements under different loading conditions in this study. Subsequently, the effects of a finite slab size, different gear configurations, a widened outer lane, a tied concrete shoulder, and a second bonded or unbonded layer were considered. Based on the principles of dimensional analysis and experimental designs, the dominating mechanistic variables were carefully identified and verified. The resulting ILLI-SLAB stresses were compared to theoretical Westergaard solutions to develop adjustment (multiplication) factors. A new regression technique (Projection Pursuit Regression) was utilized to develop prediction models to account for these theoretical differences and to instantly estimate the critical corner stresses. A practical application example showing the use of the prediction models was also provided and carefully verified using the ILLI-SLAB program.

The research findings can be practically used for various designs and analyses of jointed concrete pavements based on theoretical considerations. Not only can the use of these stress prediction models reduce the possibility of obtaining incorrect results due to the improper use of the F.E. model, but it can also reduce the complicated computation time significantly. Furthermore, the critical bending stresses can be conveniently, accurately, and the best of all --- instantly calculated through the use of these stress prediction models.

INTRODUCTION

Recently, portland cement concrete have gradually gained popularity in our highway pavement community due to its high rigidity and superior bearing capacity in order to accommodate our

dramatically increasing traffic loading. The analysis of the structural responses of pavements under a variety of loading conditions is the most crucial component when developing a mechanistic-based design procedure. Since corner breaks are one of the major structural distresses in jointed concrete pavements, this research study mainly focuses on the corner stress analysis of concrete pavements based on both sound theoretical and practical/convenient considerations.

Research Objectives

Traditionally, the Westergaard's closed-form stress solutions for a single wheel load acting on the three critical loading conditions (interior, edge, and corner) were often used in various design procedures of jointed concrete pavements. However, the actual pavement conditions are often different from Westergaard's ideal assumptions of infinite or semi-infinite slab size and full contact between the slab-subgrade interface. Besides, the effects of different gear configurations, a widened outer lane, a tied concrete shoulder, a second bonded or unbonded layer may result in very different stress responses from the Westergaard's solutions. Thus, the Westergaard's solutions have to be adjusted for these practical conditions.

These effects may be more accurately and realistically accounted through the use of a finite element (F.E.) computer program. Nevertheless, the difficulties of the required run time, the complexity of F.E. analysis, and the possibility of obtaining incorrect results due to the improper use of the F.E. model often prevent it from being used in practical pavement design. Thus, the main objectives of this research study were to develop an alternative procedure to more conveniently calculate the critical corner stresses of jointed concrete pavements with sufficient accuracy for design purposes [*9*]. Continuing research is underway to further investigate the important effects of thermal curling due to a temperature differential, warping due to a moisture gradient, and the support of the adjacent slab.

Research Approach

The ILLI-SLAB F.E. program developed at the University of Illinois over the past 15 years were used for the analysis. Based on the principles of dimensional analysis and experimental designs, several series of F.E. factorial runs over a wide range of pavement designs were carefully selected and conducted to better understand the corner structural responses of jointed concrete pavements. The resulting corner stresses were compared to the theoretical Westergaard solutions and adjustment or multiplication factors (R) were introduced to account for this

theoretical discrepancy. A new regression technique (Projection Pursuit Regression) was used to develop prediction models for the stress adjustments.

STRESS ANALYSIS OF A CONCRETE SLAB

Westergaard's Closed-Form Solutions

In the analysis of a slab-on-grade pavement system, Westergaard has presented closed-form solutions for three primary structural response variables, i.e., slab bending stress, slab deflection, and subgrade stress, due to a single wheel load based on medium-thick plate theory. Based on the assumptions of an infinite or semi-infinite slab over a dense liquid foundation (Winkler foundation), Westergaard applied a method of successive approximations and obtained the following equations for a circular corner loading condition [*14*]:

$$\pm_c = \frac{3P}{h^2}\left[1-\left(\sqrt{2}\,\frac{a}{\mathsf{a}}\right)^{0.6}\right] \qquad \text{(E. 1)}$$

Where:

σ_c = critical corner stress, [FL^{-2}];
P = total applied wheel load [F];
h = thickness of the slab [L];
a = radius of the applied load [L];
k = modulus of subgrade reaction [FL^{-3}];
a = radius of relative stiffness of the slab-subgrade system [L];

$$\mathsf{a} = \sqrt[4]{\frac{Eh^3}{12\left(1-\mu^2\right)k}} \qquad \text{(E. 2)}$$

E = modulus of elasticity of the concrete slab [FL^{-2}]; and
μ = Poisson's ratio of the concrete.

Note that primary dimensions are represented by [F] for force and [L] for length. The distance to the point of maximum stress along the corner angle bisector was found to be roughly:

$$X_1 = 2\sqrt{\sqrt{2}a^a} \cong 2.38\sqrt{a^a} \qquad \text{(E. 3)}$$

The above stress equation was derived using a simple approximate process and has been debated and led to numerous revisions such as those proposed by Bradbury, Kelly, Teller and Sutherland, Spangler, and Pickett over the years [*2*]. Despite this argument, Ioannides et al. [*3*] later has indicated that the ILLI-SLAB F.E. results closely fall between those predicted by Westergaard and Bradbury. The ILLI-SLAB stresses are the values of the **minor principal (tensile) stress** occurring at the top fiber of the slab corner. This similarity indicated that Westergaard's approximation was still fairly good.

Finite Element Solutions

In reality, jointed concrete pavements consist of many single finite concrete slabs jointed by aggregate interlock, dowel bard, or tie bars. As shown in Figure 1, traffic loading may be in the form of dual wheel, tandem axle, or tridem axle, etc. A widened outer lane may also shift the wheel loading away from Westergaard's critical loading locations. A tied concrete shoulder, a second bonded or unbonded layer may also result in different degrees of stress reductions. To account for these effects, the following relationship has been identified through many intensive F.E. studies [*5, 11*]:

$$\frac{\pm h^2}{P}, \frac{¢k^{a2}}{P}, \frac{q^{a2}}{P} = f\left(\frac{a}{a}, \frac{L}{a}, \frac{W}{a}, \frac{s}{a}, \frac{t}{a}, \frac{D_0}{a}, \frac{AGG}{k^a}, \left(\frac{h_{efft}}{h_1}\right)^2\right) \qquad \text{(E. 4)}$$

Where:

- $¢$ = deflection, [L];
- q = subgrade stress, [FL^{-2}];
- L, W = length and width of the finite slab, [L];
- s = transverse wheel spacing, [L];
- t = longitudinal axle spacing, [L];
- D_0 = offset distance between the outer face of the wheel and the slab edge, [L];
- AGG = aggregate interlock factor, [FL^{-2}];
- h_{efft} = effective thickness of two unbonded layers defined as follows, [L];

$$hefft = \left[h_1^2 + h_2^2 \left(\frac{E_2 h_2}{E_1 h_1} \right) \right]^{0.5} \qquad \text{(E. 5)}$$

h_1, h_2 = thickness of the top slab, and the bottom slab, [L]; and

E_1, E_2 = concrete modulus of the top slab, and the bottom slab, [FL^{-2}].

Since no thermal curling effect was considered in this study, the full contact assumption between the slab-subgrade interface and the principle of superposition may be applied to the analyses. Thus, the above relationship can be broken down to a series of simple analyses for each individual effect. The adjustment factors can be separately developed to account for the effect of stress reduction due to each different loading condition. Again, the ILLI-SLAB corner tensile stresses of interest were the maximum minor principal stress on the top of the slab.

FACTORIAL F.E. RUNS

The present version (March 15, 1989) [4] of the ILLI-SLAB program was successfully complied on available Unix-based workstations of the Civil Engineering Department at Tamkang University. With slight modifications to the original FORTRAN codes, a micro-computer version of the program was also successfully developed using Microsoft FORTRAN PowerStation [10] under this study.

A series of F. E. factorial runs were performed based on the dominating mechanistic variables identified. Several BASIC programs were written to automatically generate the finite element input files for future routine analyses. The F. E. mesh was generated according to the guidelines established in earlier studies [*2*] which has also been further validated under this study. More details of this analysis can be found in Reference [*7, 8, 9*]. The desired results were automatically summarized to reduce the possibility of untracked processing errors as well.

APPLICATION OF A NEW PREDICTIVE MODELING TECHNIQUE

Projection Pursuit Regression (PPR) techniques introduced by Friedman and Stuetzle [*1*] strives to model the response surface (y's) as a sum of nonparametric functions of projections of the

predictor variables (x's) through the use of local smoothing techniques. Assuming there exists a true model:

$$y = \bar{y} + \sum_{m=1}^{M_0} {}_m\alpha_m\left(a_m^T x\right) + \varepsilon \qquad \text{(E. 6)}$$

Where $x = (x_1, x_2, \cdots\cdots, x_p)^T$ denotes the vector of predictor variables, $\bar{y}$ is the expected (or mean) value of response variable, ${}_m$ is the regression coefficient, and ### is the residual or random error. The PPR algorithm strives to minimize the mean squared residuals over all possible combinations of ${}_m$, α_m, and a_m values. Conceptually, the explanatory variables x's are projected onto the direction vectors a_1, a_2, $\cdots$, a_m, to get the lengths of the projections $a_m^T x$, where m = 1, $\cdots\cdots$, M_0. An optimization technique is also used to find the best combinations of nonlinear transformations ###$_1$, ###$_2$,$\cdots$, ###$_m$ for the multidimensional response surface. $\alpha_m\left(a_m^T x\right)$ stands for the unknown nonparametric transformation functions of the projected lengths $a_m^T x$ to be estimated.

As proposed by Lee and Darter [*5, 6*], the two-step modeling approach using the PPR technique was utilized for the development of prediction models. Through the use of local smoothing techniques, the PPR attempts to model a multi-dimensional response surface as a sum of several nonparametric functions of projections of the explanatory variables. The projected terms are essentially two-dimensional curves which can be graphically represented, easily visualized, and properly formulated. Piece-wise linear or nonlinear regression techniques were then used to obtain the parameter estimates for the specified functional forms of the predictive models. This algorithm is available in the S-PLUS statistical package [*12*]. A practical predictive modeling example using this approach was presented in Reference *6*.

EFFECT OF A FINITE SLAB SIZE

Based on previous investigation [*3*], Westergaard's infinite slab assumption may be achieved if the normalized slab length (L/ª) is equal to 5.0 or more. Thus, a more conservative value of 7.0 for both L/ª and W/ª was selected to ensure infinite slab condition. The following factorial F.E. runs were conducted:

a/ª: 0.05, 0.1, 0.2, 0.3
L/ª: 2, 3, 4, 5, 6, 7

W/ℓ: 2, 3, 4, 5, 6, 7 (L/ℓ ≧ W/ℓ)

Since L/ℓ and W/ℓ are analogous, a total of 84 runs were only necessary if slab length was chosen to be greater than slab width. The resulting maximum corner stresses were obtained and compared to the Westergaard solution (as shown in equation E.1). The adjustment factor (R) for the effect of a finite slab size as shown in Figure 2 was defined as:

$$R = \frac{\pm_i}{\pm_c} \qquad \text{or} \qquad \pm_i = R \times \pm_c \tag{E. 7}$$

By using the aforementioned modeling approach, the following predictive model was developed:

$$R = \frac{\pm_i}{\pm_c} = 1.030 + 0.030\Phi_1 + 0.045\Phi_2$$

$$\Phi_1 = 92.145 - 149.276(A1) + 59.747(A1)^2$$

$$\Phi_2 = \begin{cases} -6.034 + 23.128(A2) - 22.022(A2)^2 & if \quad A2 \le 0.6 \\ -0.117 + 0.375(A2) & if \quad 0.6 < A2 \end{cases}$$

$$A1 = 0.8272x1 - 0.1219x2 + 0.0002x3 + 0.5485x4$$

$$A2 = -0.9034x1 + 0.2973x2 - 0.0118x3 - 0.3088x4$$

$$X1 = [x1, x2, x3, x4] = \left[\frac{a}{\ell}, \frac{L}{\ell} + \frac{W}{\ell}, \frac{L}{\ell} \times \frac{W}{\ell}, \sqrt{\frac{L}{\ell}} + \sqrt{\frac{W}{\ell}}\right] \tag{E. 8}$$

Statistics:

N = 84, R^2 = 0.980, SEE = 0.0081, CV = 0.79%

Limits:

$0.05 \le a/\ell \le 0.3, 2 \le L/\ell \le 7, W/\ell \le L/\ell$

Note that N is the number of data points, R^2 is the coefficient of determination, SEE is the standard error of estimates, and CV is the coefficient of variation. Figure 2 also shows the result of projection modeling, where A1, A2, ϕ1, and ϕ2 were labeled as “ATX1”, “ATX2”, “1st Projected Term,” and “2nd Projected Term,” respectively. This prediction model is also applicable to a larger slab when the upper bound value of 7.0 is used for the normalized slab length or width (L/ℓ, W/ℓ).

GEAR CONFIGURATIONS

Adjustment factors were introduced to convert different gear configurations (multiple wheels or axles) to a single wheel / single axle loading condition. The adjustment factor was defined as:

$$R = \frac{\pm_s}{\pm_{s=0}} \quad \text{or} \quad R = \frac{\pm_t}{\pm_{t=0}} \qquad \text{(E. 9)}$$

Where:

σ_s, σ_t = maximum corner stresses for multiple wheels and multiple axles, respectively, [FL^{-2}]; and

$\sigma_{s=0}$, $\sigma_{t=0}$ = maximum corner stresses for multiple wheels when s=0 and multiple axles when t=0, respectively, [FL^{-2}].

To eliminate the effect of a finite slab size from this analysis, the slab size has to be large enough to assure infinite slab conditions when the wheel spacing (s) and/or axle spacing (t) increases. Thus, a large value of 10 was assigned to the normalized slab size (L/ℓ and W/ℓ) for all the following factorial F.E. runs:

a/ℓ : 0.05, 0.1, 0.2, 0.3, 0.4

s/ℓ, t/ℓ : 0.0 - 4.0, by 0.2 increments

Also note that the largest normalized wheel spacing (s/ℓ) and normalized axle spacing (t/ℓ) values were chosen to be 4.0, which also agrees with the 4ℓ infinite slab size criteria observed by Ioannides et. al. [*3*] for maximum corner stresses. The following three cases of gear configurations were analyzed in this study:

(1) dual wheel / single axle,
(2) single wheel / tandem axle, and
(3) single wheel / tridem axle.

As shown in Figure 1, the effects of other different variations of gear configurations such as dual wheel / tridem axle, and dual wheel / tandem axle may be derived based on the principle of superposition. These combination effects will be illustrated and further validated in a case study.

Dual Wheel / Single Axle

As shown in Figure 3, the adjustment factors (R) could be less than 1/2 for this case. If a conservative lower bound of 1/2 is selected for design purposes, the effect will be equivalent to that due to a single wheel load when s/ increases to 1.5 or higher. The maximum tensile stress location occurred on the top of the slab corner had similar trends with Westergaard's equation, a distance of $x' = 2.38\sqrt{a^a}$ along the corner angle bisector, for a single wheel load. The following predictive model (as also shown in Figure 3) was developed:

$$R = 0.6028 + 0.1338\,\Phi_1 + 0.00687\Phi_2$$

$$\Phi_1 = \begin{cases} 0.548 + 0.861(A1) + 0.208(A1)^2 + 0.0176(A1)^3 & \text{if } A1 \le 2.0 \\ 2.963 + 4.594(A1) + 2.249(A1)^2 + 0.407(A1)^3 & \text{if } A1 > -2.0 \end{cases}$$

$$\Phi_2 = \begin{cases} -0.382 - 0.364(A2) & \text{if } A2 \le -0.04 \\ 1.109 + 39.675(A2) & \text{if } A2 < -0.04 \end{cases}$$

$$A1 = -0.986x1 + 0.00507x2 + 0.164x3 - 0.0121x4$$

$$A2 = -0.0412x1 - 0.918x2 + 0.393x3 + 0.00129x4$$

$$X = (x1, x2, x3, x4) = \left(\frac{s}{a}, \frac{a}{a}, \frac{s \cdot a}{a^2}, \frac{s}{a}\right) \qquad \text{(E. 10)}$$

Statistics : N=105 , R^2=1.000, SEE=0.0026

Limits : $0.05 \le (a/a) \le 0.4$, $0 \le (s/a) \le 4$

Single Wheel / Tandem Axle

For an infinite slab size in both x and y directions, this case is analogous to the above dual wheel / single axle case. Thus, the adjustment factor may be obtained by substituting the normalized axle spacing (t/a) into the normalized wheel spacing (s/a) of the above prediction equation (E.9).

Single Wheel / Tridem Axle

As shown in Figure 4, the adjustment factor (R) approached to a lower bound value of 1/3 when the normalized axle spacing (t/) reached 1.7 or higher. In other words, the resulting

maximum corner stress of a single wheel / tridem axle is equivalent to that due to a single wheel load. Despite the fact that the maximum tensile stress location on the top of the slab varied from case to case, the maximum stress values were used for the model development. The following prediction model (as also shown in Figure 4) was developed:

$$R = 0.4468 + 0.1679\Phi_1$$

$$\Phi_1 = \begin{cases} -0.154 + 0.346(A1) + 0.0986(A1)^2 + 0.0101(A1)^3 & \text{if } A1 \le 2.5 \\ 3.169 + 5.426(A1) + 2.880(A1)^2 + 0.528(A1)^3 & \text{if } A1 > 2.5 \end{cases}$$

$$A1 = -0.9999x1 + 0.00576x2 - 0.0122x3$$

$$X = (x1, x2, x3) = \left(\frac{t}{a}, \frac{a}{a}, \frac{t}{a}\right) \qquad \text{(E. 11)}$$

Statistics: N= 105, R^2=0.996, SEE=0.0103
Limits: $0.05 \le (a/a) \le 0.4$, $0 \le (t/a) \le 4$

Effects of Wheel and Axle Spacings

In summary, the results showed that the adjustment factors will reduce to 1/2 for a dual wheel or a tandem axle, and reduce to 1/3 for a tridem axle when the wheel spacing (s) or axle spacing (t) is greater than 1.5a or 1.7a. Thus, a conservative s or t value of 1.7a (or even 2.0a), which is approximately equal to one-half of the 4a infinite slab size criteria observed by Ioannides [3], may be used for design purposes. Under such conditions, the influences of other wheels and axles to the critical corner stresses are minimal and may be neglected.

A WIDENED OUTER LANE

The following factorial F.E. runs were conducted to account for the effect of a widened outer lane, where D_o is the offset distance between the outer face of the wheel and the slab edge:

a/a: 0.05, 0.1, 0.2, 0.3, 0.4
D_o /a: 0 - 4, by 0.2 increments

A relative large value of 12 was used for the normalized slab length (L/ª) and normalized slab width (W/ª) to assure infinite slab conditions for all the factorial runs. The adjustment factor (R) for the stress reduction was defined as follows:

$$R = \frac{\pm_D}{\pm_{D=0}} \qquad \text{(E. 12)}$$

Where:

σ_D = maximum corner stress of a slab with a widened outer lane, [FL^{-2}];

$\sigma_{D=0}$ = maximum corner stress of a slab without a widened outer lane, [FL^{-2}];

When D_o /ª gradually increases, the location of critical bending stresses will shift from the top of the slab corner to the bottom of the slab edge (or transverse joint). Under this study, only the maximum tensile stress occurred on the top of the slab corner was considered. As shown in Figure 5, the maximum corner stress decreases when D_o /ª increases. The following prediction model (as also shown in Figure 5) was developed:

$$R = 0.4429 + 0.1853\Phi_1 + 0.0335\Phi_2$$

$$\Phi_1 = \begin{cases} 0.786 + 1.434(A1) + 0.463(A1)^2 + 0.0531(A1)^3 & if \quad A1 \geq -1 \\ 3.144 + 8.390(A1) + 7.674(A1)^2 + 2.667(A1)^3 & if \quad A1 < -1 \end{cases}$$

$$\Phi_2 = \begin{cases} 0.581 + 4.406(A2) + 16.204(A2)^2 & if \quad A2 \geq 0.1 \\ 0.408 + 4.209(A2) & if \quad A2 < 0.1 \end{cases}$$

$$A1 = -0.780x1 - 0.0597x2 + 0.622x3 - 0.00333x4$$

$$A2 = -0.0524x1 - 0.781x2 + 0.622x3 - 0.00737x4$$

$$X = (x1, x2, x3, x4) = \left(\frac{D_0}{a}, \frac{a}{a}, \frac{D_0 \cdot a}{a^2}, \frac{D_0}{a}\right) \qquad \text{(E. 13)}$$

Statistics : N= 105, R^2=0.998, SEE=0.0086

Limits : $0.05 \leq (a/ª) \leq 0.4$, $0 \leq (D_0/ª) \leq 4$

A TIED CONCRETE SHOULDER

The effect of a tied concrete shoulder was considered in this case. The following factorial F.E.

runs were conducted:

a/ : 0.05, 0.1, 0.2, 0.3, 0.4
AGG/k : 0, 5, 50, 500, 1000, 5000, 10000, 20000, 30000, 50000

A relative large value of 10 was used for the normalized slab length (L/ª) and normalized slab width (W/ª) to eliminate the effect of finite slab size for all the factorial runs. The adjustment factor (R) for the stress reduction as shown in Figure 6 was defined as follows:

$$R = \frac{\pm_{AGG}}{\pm_{AGG=0}} \qquad \text{(E. 14)}$$

Where:

σ_{AGG} = maximum corner stress of a slab with a tied concrete shoulder, [FL^{-2}]; and
$\sigma_{AGG=0}$ = maximum corner stress of a slab without a tied concrete shoulder, [FL^{-2}].

When AGG/k = 0, the influence of a tied concrete shoulder may be neglected. On the other hand, an edge load condition may be resulted if AGG/k increases dramatically. Under such conditions, the critical tensile stress is located at the bottom of the slab (or transverse joint) rather than on the top of the slab corner. Under this study, only the maximum corner stress was considered. The following prediction model (as also shown in Figure 6) was developed for the adjustment factors:

$$R = 0.7543 + 0.1887\Phi_1 + 0.01840\Phi_2$$

$$\Phi_1 = \begin{cases} 12.940 + 15.138(A1) + 5.305(A1)^2 + 0.604(A1)^3 & \text{if } A1 \le -2.55 \\ 1.321 + 0.154(A1) + 0.760(A1)^2 + 0.965(A1)^3 + 0.212(A1)^4 & \text{if } A1 > -2.55 \end{cases}$$

$$\Phi_2 = 0.324 + 7.064(A2) + 7.003(A2)^2$$

$$A1 = -0.531x1 + 0.636x2 - 0.560x3 + 0.00192x4$$

$$A2 = -0.176x1 - 0.682x2 + 0.710x3 + 0.00639x4$$

$$X = (x1, x2, x3, x4) = \left(LAGG, \frac{a}{a}, \frac{LAGG * a}{a}, \frac{LAGG}{a}\right)$$

$$where, LAGG = \log_{10}\left(1 + \frac{AGG}{k^a}\right) \qquad \text{(E. 15)}$$

Statistics: N=50, R^2=1.000, SEE=0.0043
Limits: $0.05 \le (a/a) \le 0.4$, $0 \le (AGG/k^a) \le 50000$

A SECOND BONDED OR UNBONDED LAYER

A second bonded or unbonded layer may be constructed between the top slab and the subgrade of a jointed concrete pavement. For a fully unbonded case, both the top and bottom layers may be treated as a single layer with the effective thickness as defined in equation (E.5) [*11, 13*]. Thus, the following factorial F.E. runs were conducted:

a/ : 0.05, 0.1, 0.2, 0.3, 0.4
(hefft/h1)^2 : 1.0 - 2.0, by 0.1 increments

The adjustment factor (R) as shown in Figure 7 was defined as:

$$R = \frac{\pm_{h2}}{\pm_{h2=0}} \qquad \text{(E. 16)}$$

Where:

σ_{h2} = maximum corner stress of a slab with a second unbonded layer, [FL^{-2}]; and

$\sigma_{h2=0}$ = maximum corner stress of a slab without a second unbonded layer, [FL^{-2}].

The following prediction model (as also shown in Figure 7) for the adjustment factor was developed:

$$R = 0.72692 + 0.14272\Phi_1 + 0.00933\Phi_2$$

$$\Phi_1 = \begin{cases} 3.31765 + 2.4036(A1) & \text{if } A1 \le -1.4 \\ 5.72684 + 4.10244(A1) & \text{if } A1 > -1.4 \end{cases}$$

$$\Phi_2 = \begin{cases} 14.535 - 20.351(A2) + 5.986(A2)^2 & \text{if } A2 \le 1.2 \\ 1.619 - 8.367(A2) + 4.877(A2)^2 & \text{if } A2 > 1.2 \end{cases}$$

$$A1 = 0.11914x1 - 0.99288x2$$

$$A2 = 0.65518x1 + 0.75547x2$$

$$X = [x1, x2] = \left[\frac{a}{a}, \left(\frac{h_{efft}}{h1} \right)^2 \right] \qquad \text{(E. 17)}$$

Statistics : N=55 , R^2=0.998, SEE=0.0066

Limits : $0.05 \le (a/a) \le 0.4$, $1 \le (h_{efft}/h_1)^2 \le 2$

As for the effect of a second bonded layer, an equivalent layer based on the concept of transformed section could be determined. The conversion procedures and equations can be found elsewhere in the literature [*11, 13*].

CASE STUDY AND VERIFICATION

Suppose there exists a jointed concrete pavement (in Figure 8) with the following characteristics: (Note: 1 in. = 2.54 cm, 1 psi = 0.07 kg/cm^2, 1 pci = 0.028 kg/cm^3, 1 kip = 454 kg)

1. a two-layer unbonded slab
2. finite slab size: L = 188 in., W = 147 in.
3. thickness of the top and the bottom layers: h_1 = 10 in., h_2 = 6 in.
4. concrete modulus of the top and the bottom layers: E_1 = 6.0E+06 psi, E_2 = 2.01E+06 psi
5. Poisson's ratio of the top and the bottom layers: $\mu_1 = \mu_2 = 0.15$
6. self-weight of the top and the bottom slabs: $\gamma_1 = \gamma_2 = 0.085$ pci
7. modulus of subgrade reaction: k = 500 pci
8. a tied concrete shoulder: aggregate interlock factor (AGG) = 5000 psi
9. loading conditions: a dual wheel / tridem axle (i.e., a total of 6 wheels)
   loaded area = 7.5 in. x 10 in. for each wheel
   (radius of the loaded area, a = 4.88 in.)
   wheel spacing, s = 15 in.
   axle spacing, t = 30 in.
   tire pressure, p = 100 psi
10. an offset distance due to a widened outer lane, D_o = 12 in.

The following steps showing the use of the proposed prediction models was used to estimate the maximum minor principal (tensile) stress on the top of the slab corner. More details of the calculations were given in Table 1 and Table 2.

1. **<u>The effect of a finite slab size</u>**: a/ℓ = 0.153, L/ℓ = 5.91, W/ℓ = 4.62, and the adjustment factor is equal to R = 1.035 using equation (E.8).
2. **<u>Gear configurations</u>**: Decomposing the dual wheel / tridem axle into the combination of a dual wheel / single axle and a single wheel / tridem axle. s/ℓ = 0.472, t/ℓ = 0.943, and thus the adjustment factors (R) for both cases are 0.762 and 0.459 using equations (E.10) and (E.11), respectively. The adjustment factor for this case (a dual wheel / tridem axle) is equal to 0.762 * 0.459 = 0.350.

3. **A widened outer lane**: $D_o / a = 0.377$, and R = 0.667 using equation (E.13).
4. **A tied concrete shoulder**: $AGG/k^a = 0.314$, and R = 0.998 using equation (E.15).
5. **A second unbonded layer**: $a/a = 0.149$, $(hefft/h1)^2 = 1.07$, and then the adjustment factor is equal to R = 0.941 using equation (E.17).
6. **Estimated maximum corner stress**: The total applied load of these 6 wheels was equal to P = 45 kips, thus the Westergaard's corner stress before adjustments was 810 psi using equation (E.1). The overall adjustment factor can be determined by multiplying the adjustment factors of items (1) to (5) together, i.e., R = 1.035 * 0.350 * 0.667 * 0.998 * 0.941 = 0.227. Thus, the estimated maximum corner stress for this case study was equal to 810 * 0.227 = 183.9 psi
7. **Comparison to ILLI-SLAB stresses**: The estimated maximum minor principal (tensile) stress (183.9 psi) was compared to the resulting ILLI-SLAB stress (134 psi). Thus, further investigations of various combinations of individual loading conditions were conducted and summarized in Table 2. Apparently, fairly good agreements were achieved for each individual case. Since the critical location of minor principal stress changes from case to case, the resulting combined stress estimations were usually in the conservative side. To resolve this discrepancy, the location of critical stress occurrence has to be further investigated.

CONCLUSIONS AND RECOMMENDATIONS

An alternative procedure for the determination of the critical corner stresses of jointed concrete pavements was developed under this study. The effects of a finite slab size, different gear configurations, a widened outer lane, a tied concrete shoulder, a second bonded or unbonded layer were considered. The major research findings of this study are summarized as follows:

1. To more accurately estimate the corner stress of a jointed concrete pavement, the effect of a finite slab size has to be considered.
2. Adjustment factors (R) were introduced and carefully selected to account for the effects of different gear configurations. The ranges of R were between 1 and 1 / N for N wheels. The influences of other wheels and axles to the critical corner stress are minimal and may be neglected if the normalized wheel spacing (s/a) and the normalized axle spacing (t/a) exceed 1.5 or 1.7. Thus, a conservative s or t value of $1.7a$ (or even $2.0a$), which is approximately equal to one-half of the $4a$ infinite slab size criteria observed by Ioannides, may be used for design purposes.

3. When the effect of a widened outer lane (or the normalized offset distance D_o /ª) gradually increases, the location of critical bending stresses will shift from the top of the slab corner to the bottom of the slab edge (or transverse joint). Under this study, only the maximum tensile stress occurred on the top of the slab corner was considered. The maximum corner stress decreases when D_o /ª increases.
4. When AGG/k = 0, the influence of a tied concrete shoulder may be neglected. On the other hand, an edge load condition may be resulted if AGG/k increases dramatically. Under such conditions, the critical tensile stress is located at the bottom of the slab (or transverse joint) rather than on the top of the slab corner. Under this study, only the maximum corner stress was considered.
5. The effect of a second unbonded layer may be determined by a stress adjustment factor. The concept of transformed section may be applied to account for the effect of a second bonded layer.
6. Prediction models were developed for each of the individual effect. The principle of superposition may be applied to account for these combination effects.

Several improvements to the proposed alternative procedure for corner stress determination may be necessary. Recommendations for further research are discussed as follows:

1. The location of critical stress occurrence and the effect of different subgrade models should be further investigated.
2. It is still desirable to compare the resulting ILLI-SLAB stresses with actual field measurements to further validate the accuracy of the F.E. model. Despite the fact that ILLI-SLAB results have been field-validated many times in the literature with very good agreements. [*5, 13*]
3 The adjustment factors were developed based on loading only condition. To more realistically describe actual field conditions, the effects of thermal curling due to a temperature differential, warping due to a moisture gradient, and the support of the adjacent slab, especially the load transfer efficiency of doweled jointed concrete pavements, will be further investigated in the on-going research.

ACKNOWLEDGMENTS

This research was sponsored by the National Science Council, the Republic of China, under the grant No. NSC84-2211-E032-008. Additional financial support provided by Tamkang University and very helpful recommendations provided by Dr. Ho-Shong Hou and Professor Pien-Sien Lin are very much appreciated. Previous research work conducted by Dr. R. A. Salsilli also provide very fruitful ideas for the successful accomplishment of this study.

REFERENCES

1. Friedman, J. H. and W. Stuetzle, "Projection Pursuit Regression," Journal of the American Statistical Association, Vol. 76, 1981, pp. 817-823.
2. Ioannides, A. M., "Analysis of Slabs-on-Grade for a Variety of Loading and Support Conditions," Ph.D. Thesis, University of Illinois, Urbana, 1984.
3. Ioannides, A. M., M. R. Thompson and E. J. Barenberg, "Westergaard Solutions Reconsidered," Transportation Research Record 1043, Transportation Research Board, National Research Council, Washington, D. C., pp. 13-23, 1985.
4. Korovesis, G. T., "Analysis of Slab-on-Grade Pavement Systems Subjected to Wheel and Temperature Loadings," Ph.D. Thesis, University of Illinois, Urbana, 1990.
5. Lee, Y. H., "Development of Pavement Prediction Models," Ph.D. Thesis, University of Illinois, Urbana, 1993.
6. Lee, Y. H., and M. I. Darter, "New Predictive Modeling Techniques for Pavements," Transportation Research Record 1449, Transportation Research Board, National Research Council, Washington, D.C., 1994, pp. 234-245.
7. Lee, Y. H., Y. M. Lee, and J. H. Chen, "Theoretical Investigation of Corner Stress in Concrete Pavements Using Dimensional Analysis," Final Report (In Chinese), National Science Council, Grant No. NSC83-0410-E032-009 and NSC84-2211-E032-022, Taiwan, August 1995.
8. Lee, Y. H. and Y. M. Lee, "Development of New Stress Analysis and Thickness Design Procedures for Jointed Concrete Pavements," Final Report - First Phase (In Chinese), National Science Council, Grant No. NSC84-2211-E032-008, Taiwan, August 1995.
9. Lee, Y. M., "Stress Analysis of Jointed Concrete Pavements," M.S. Thesis (In Chinese), Tamkang University, Tamsui, Taipei, June 1995.
10. Microsoft, "Microsoft FORTRAN PowerStation Professional Development System," User's and Reference Manuals, Microsoft Taiwan Corp., 1994.
11. Salsilli-Murua, R. A., "Calibrated Mechanistic Design Procedure for Jointed Plain Concrete

Pavements," Ph.D. Thesis, University of Illinois, Urbana, 1991.

12. Statistical Sciences, Inc., S-PLUS for Windows: User's and Reference Manuals, Ver. 3.1, Seattle, Washington, 1993.
13. Tabatabaie-Raissi, A. M., "Structural Analysis of Concrete Pavement Joints," Ph.D. Thesis, University of Illinois, Urbana, 1978.
14. Westergaard, H. M., "Computation of Stresses in Concrete Roads," Proceeding of the Fifth Annual Meeting, Vol. 5, Part I, Highway Research Board, National Research Council, 1925 (Published in 1926), pp. 90-112.

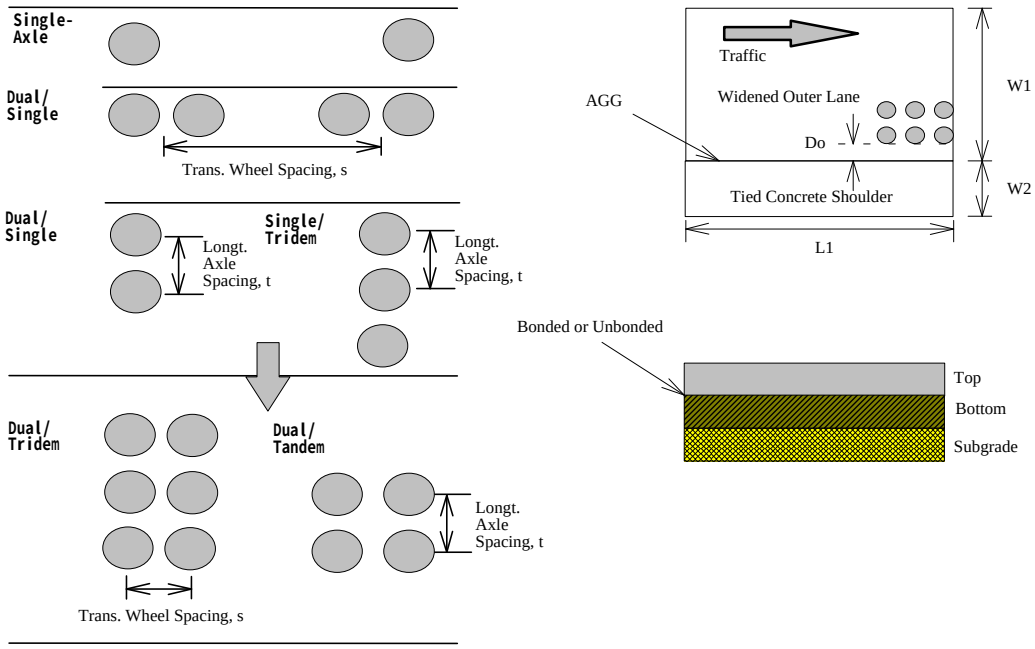

Figure 1 - Various Conditions of Jointed Concrete Pavements

Figure 2 - Adjustment for the Effect of a Finite Slab Size

Figure 3 - Adjustment Factor of a Dual Wheel / Single Axle

Figure 4 - Adjustment Factor of a Single Wheel / Tridem Axle

Figure 5 - Adjustment Factor of a Widened Outer Lane

Figure 6 - Adjustment Factor of a Tied Concrete Shoulder

Figure 7 - Adjustment Factor of a Second Unbonded Layer

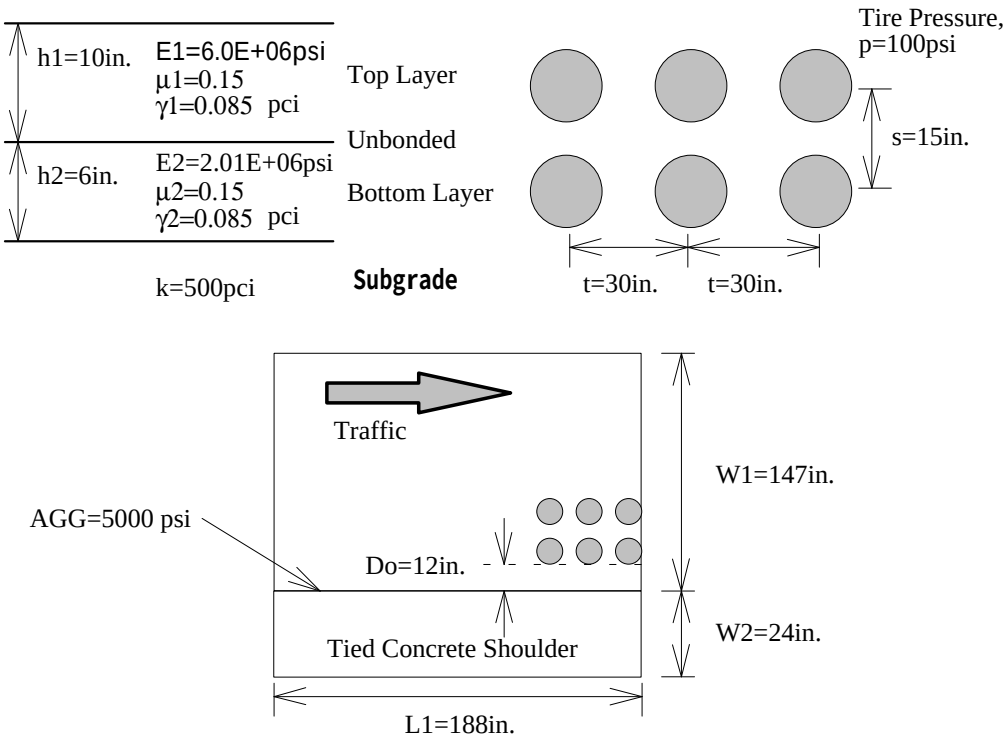

Figure 8 - A Case Study for Validation

Table 1 - Stress Calculations for the Case Study

Dual-Single		**Single-Tridem**		**Widened Outer Lane**		**Tied Concrete Shoulder**		**Second Unbonded Layer**		**Finite Slab Size**		**Results**	
a	4.88	a	4.88	a	4.88	AGG	5000	a/*l*	0.149	L	188	P	7500
l	31.8	t	30	*l*	31.8	k	500	(hefft/h1)^2	1.072	W	147	h	10
s	15	t/*l*	0.943	Do	12	*l*	31.8	A1	-1.047	*l*	31.8	a/*l*	0.153
s/*l*	0.472	a/*l*	0.153	Do/*l*	0.377	a	4.88	A2	0.908	L/*l*	5.912	N	6.000
a/*l*	0.153	t/a	6.148	a/*l*	0.153	AGG/k*l*	0.314	Φ1	1.432	W/*l*	4.623	Wes. Stress	810.2
s*a/*l*^2	0.072	A1	-1.017	Do*a/*l*^2	0.058	LAGG	0.119	Φ2	0.994	a/*l*	0.153	Rtotal	0.227
s/a	3.074	Φ1	0.074	Do/a	2.459	a/*l*	0.153	R	0.941	(W/*l*)+(L/*l*)	10.535	Max. Stress	183.6
A1	-0.490	R	0.459	A1	-0.276	LAGG*a/l	0.018			(W/*l*)*(L/*l*)	27.329		
A2	-0.128			A2	-0.082	LAGG*l/a	0.774			(W/*l*)^0.5 + (L/*l*)^0.5	4.581	ILLI-SLAB StressS	134
Φ1	1.205			Φ1	1.358	A1	0.026			A1	1.361		
Φ2	-0.335			Φ2	-0.834	A2	-0.108			A2	1.256		
R	0.762			R	0.667	Φ1	1.326			Φ1	-0.353		
						Φ2	-0.355			Φ2	0.354		
						R	0.998			R	1.035		

Note: L, W, h, a, *l,* s, t, and Do are in inches. P is in pounds, k is in pci, AGG and stress are in psi.

Table 2 - Various Cases of Stress Estimations and Comparisons

		No Second Unbonded Layer			With Second Unbonded Layer		
		R	Estimated Stress	ILLI-SLAB Stress	R	Estimated Stress	ILLI-SLAB Stress
No Widened Outer Lane	Dual	0.789	213.0	213.5	0.742	200.3	200.9
	Tridem	0.475	192.4	199.2	0.447	181.0	187.7
	Dual-Tridem	0.362	293.2	279.2	0.341	276.2	265.1
With Widened Outer Lane	Dual	0.526	142.0	148.3	0.495	133.7	140.3
	Tridem	0.317	128.4	115.2	0.298	120.7	109.5
	Dual-Tridem	0.241	195.2	165.3	0.227	183.9	157.5

Key Words:

Concrete Pavements, Stress Analysis, Loading, Predictive Models, Pavement Deign, Projection Pursuit Regression (PPR), Mechanistic Design

Figure 1 - Various Conditions of Jointed Concrete Pavements

Figure 2 - Adjustment for the Effect of a Finite Slab Size

Figure 3 - Adjustment Factor of a Dual Wheel / Single Axle

Figure 4 - Adjustment Factor of a Single Wheel / Tridem Axle

Figure 5 - Adjustment Factor of a Widened Outer Lane

Figure 6 - Adjustment Factor of a Tied Concrete Shoulder

Figure 7 - Adjustment Factor of a Second Unbonded Layer